Indirect Determination of the Higgs Mass Through Electroweak Radiative Corrections

A. Freitas
Fermi National Accelerator Laboratory, Batavia, IL 60510-500, USA
M. Awramik
DESY, Platanenallee 6, D-15738 Zeuthen, Germany;
Institute of Nuclear Physics PAS, Radzikowskiego 152, PL-31342 Cracow, Poland
M. Czakon
Institut für Theoretische Physik und Astrophysik, Universität Würzburg, Am Hubland, D-97074 Würzburg, Germany;
Institute of Physics, University of Silesia, Uniwersytecka 4, PL-40007 Katowice, Poland

Electroweak precision observables allow stringent tests of the Standard Model at the quantum level and imply interesting bounds on the mass of the Higgs boson through higher-order loop effects. Very significant constraints come especially from the determination of the mass of the W boson and from the effective leptonic weak mixing angle. After shortly reviewing the status of theoretical computations of the W mass, the new calculation of two-loop corrections with closed fermion loops to the effective leptonic weak mixing angle is discussed in detail. The phenomenological implications of the new result are analyzed including an estimate of remaining uncertainties.

1. INTRODUCTION

In recent years, the Standard Model of electroweak interactions has been confirmed experimentally with outstanding success. Not only was almost all the particle content discovered at accelerator experiments, but their properties and interactions have been measured with high precision, in agreement with the model prediction. The only missing piece is the Higgs boson, which is responsible for electroweak symmetry breaking. However, even today we can obtain meaningful constraints on the Higgs boson mass from electroweak precision measurements. Due to the impressive accuracy of some of these experimental results, they are sensitive to electroweak radiative corrections at the next-to-leading (NLO) and sometimes next-to-next-to-leading (NNLO) level, and thus depend on the impact of the Higgs boson entering in the loops.

Two of the most important quantities in this respect are the mass of the W boson, $M_{\rm W}$ and the sine of the leptonic effective weak mixing angle $\sin^2\theta_{\rm eff}^{\rm lept}$. The W-boson mass can be inferred from the muon decay constant G_μ, which is generated through virtual W-boson exchange, so that $G_\mu \propto 1/M_{\rm W}^2$. The effective weak mixing angle, on the other hand, reflects the ratio of the vector and axial-vector couplings, v_f and a_f, of the Z boson to fermions (f) at the Z boson pole:

$$\sin^2\theta_{\rm eff}^f = \frac{1}{4}\left(1 + {\rm Re}\frac{v_f}{a_f}\right). \tag{1}$$

Since these couplings can be measured most precisely for leptons, the *leptonic* effective weak mixing angle $\sin^2\theta_{\rm eff}^{\rm lept}$ is usually taken as a reference.

The current experimental world average for the W-boson mass is $M_{\rm W} = (80.425 \pm 0.034)$ GeV [1]. Recently, a lot of progress has been made towards establishing accurate theoretical prediction for $M_{\rm W}$. The best result [2] includes the complete two-loop corrections [3, 4] and some three-loop contributions [5, 6]. The remaining theoretical error is estimated to be $\delta M_{\rm W} \sim 4$ MeV, which is well below the current experimental uncertainty. Still, the electroweak two-loop corrections total to ~ 30 MeV and are thus mandatory for electroweak precision analyses.

The effective weak mixing angle $\sin^2\theta_{\rm eff}^{\rm lept}$ is mainly derived from various asymmetries measured around the Z boson peak at e^+e^- colliders after subtraction of QED effects. The current experimental accuracy, $\sin^2\theta_{\rm eff}^{\rm lept} =$

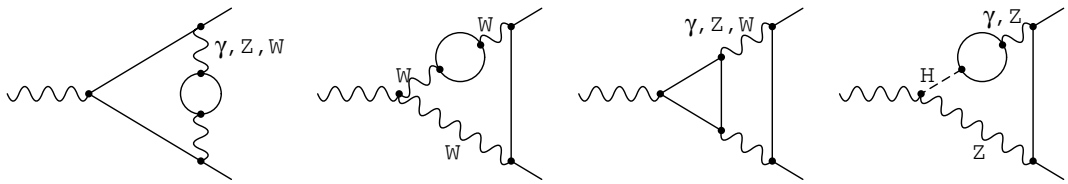

Figure 1: Genuine two-loop Zl^+l^- vertex diagrams contributing to $\sin^2\theta_{\rm eff}^{\rm lept}$.

0.23150 ± 0.00016 [1] implies strong indirect constraints on the allowed range for the Higgs boson mass $M_{\rm H}$. Therefore it is important to develop precise theoretical calculations for this quantity.

Usually, $\sin^2\theta_{\rm eff}^{\rm lept}$ is computed as a function of the electromagnetic coupling α, the muon constant G_μ and the masses of the Z boson, $M_{\rm Z}$, and the top quark, $m_{\rm t}$ (other fermion masses are numerically irrelevant). As explained before, $M_{\rm W}$ is calculated from G_μ, but in addition to these corrections, the computation of $\sin^2\theta_{\rm eff}^{\rm lept}$ involves the corrections to the Z vertex form factors. The latter are expressed by the quantity $\kappa = 1 + \Delta\kappa$, in such a way that the effective weak mixing angle can also be written as:

$$\sin^2\theta_{\rm eff}^{\rm lept} = \left(1 - M_W^2/M_Z^2\right)(1 + \Delta\kappa)\,, \tag{2}$$

and at tree-level, $\Delta\kappa = 0$. Higher-order corrections to $\sin^2\theta_{\rm eff}^{\rm lept}$ have been under extensive theoretical study over the last two decades. Besides the one-loop result [7, 8], two- and three-loop QCD corrections are available [5, 9, 10], but for the electroweak two-loop contributions only partial results were known. By means of a large mass expansion in the heavy top quark mass, the formally leading $\mathcal{O}(\alpha^2 m_{\rm t}^4)$ [11, 12] and next-to-leading $\mathcal{O}(\alpha^2 m_{\rm t}^2 M_{\rm Z}^2)$ [13] terms were computed. A part of the missing two-loop contributions was incorporated by the complete electroweak two-loop corrections to $M_{\rm W}$ [3, 4]. While these corrections effected a shift in $M_{\rm W}$ of 4 MeV compared to the previously known $\mathcal{O}(\alpha^2 m_{\rm t}^2 M_{\rm Z}^2)$ contributions, the induced shift in $\sin^2\theta_{\rm eff}^{\rm lept}$ was very sizable, $\delta\sin^2\theta_{\rm eff}^{\rm lept} = 8\times 10^{-5}$, thus implying that the missing two-loop terms in the form factor $\Delta\kappa$ can be of similar order.

2. ELECTROWEAK TWO-LOOP CORRECTIONS TO $\sin^2\theta_{\rm eff}^{\rm lept}$

As a first step towards completing the electroweak two-loop corrections to $\sin^2\theta_{\rm eff}^{\rm lept}$, results for the fermionic (i.e. diagrams with closed fermion loops) two-loop corrections were presented recently [14]. The genuine two-loop vertex diagrams are represented by the generic topologies in Fig. 1. Higher-order corrections to the process $e^+e^- \to f\bar{f}$ near the Z pole can be consistently computed by performing an expansion of the amplitude around the complex pole $\mathcal{M}_{\rm Z}^2 = M_{\rm Z}^2 - iM_{\rm Z}\Gamma_{\rm Z}$,

$$\mathcal{A}[e^+e^- \to f\bar{f}] = \frac{R}{s - \mathcal{M}_{\rm Z}^2} + S + (s - \mathcal{M}_{\rm Z}^2)S' + \ldots \tag{3}$$

Here $\Gamma_{\rm Z}$ is the Z decay width. After subtracting contributions from s-channel photon exchange and γ-Z interference, the vertex corrections form factor at NNLO is derived to be

$$\kappa_{\rm f}^{(2)} = \left.\frac{\hat{a}_{\rm f}^{(2)}\, v_{\rm f}^{(0)}\, a_{\rm f}^{(0)} - \hat{v}_{\rm f}^{(2)}\,(a_{\rm f}^{(0)})^2 - (\hat{a}_{\rm f}^{(1)})^2\, v_{\rm f}^{(0)} + \hat{a}_{\rm f}^{(1)}\,\hat{v}_{\rm f}^{(1)}\, a_{\rm f}^{(0)}}{(a_{\rm f}^{(0)})^2(a_{\rm f}^{(0)} - v_{\rm f}^{(0)})}\right|_{s=M_{\rm Z}^2}, \tag{4}$$

where the superscripts in parentheses indicate the loop order. In this quantity, IR-divergencies from QED contributions drop out, which involves a delicate interplay between one- and two-loop terms in the form factors. The UV-divergencies are cancelled by on-shell renormalization. The relevant counterterms are derived using the methods of Ref. [3].

The new part of this work is the computation of the two-loop $Zf\bar{f}$ vertex corrections, which are treated with two independent technical methods. The first method uses large mass expansions for the diagrams with internal

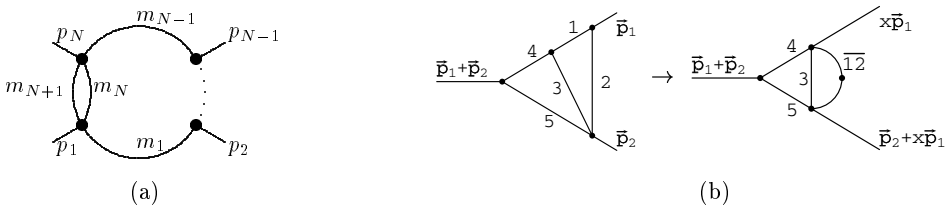

Figure 2: (a) General representation of a two-loop scalar diagram with self-energy sub-loop. (b) Reduction of triangle sub-loop to self-energy sub-loop by means of Feynman parameters.

top-quark lines and the differential equation method for diagrams with only light fermions $f \neq t$, the masses of which are neglected. Contrary to previous work [13], the expansion in $x = M_Z^2/m_t^2$ is performed to high precision, by executing the series to the order x^{10}, reaching an overall relative precision of $\sim 10^{-5}$ of the final result. The coefficients of the expansion are 2-loop tadpole and 1-loop vertex diagrams, which can be evaluated efficiently with well-known analytical formulae. The contributions from diagrams without top-quark propagators involve only two independent scales, M_Z and M_W, allowing a fully analytical treatment. Even for the limited set of diagrams with closed fermions loops, a large number of scalar integrals with non-trivial structures in the numerator are involved. They can be reduced to a set of scalar master integrals by using integration-by-parts identities [15]. Owing to size of the linear equation system associated with this reduction procedure, the algorithm has been implemented in the dedicated C++ library DiaGen/IdSolver [16], which performs the necessary steps in a highly automized way. Analytical results for these master integrals are obtained by the differential equation method [17]. This is illustrated by the following example,

$$p^2 \frac{\mathrm{d}}{\mathrm{d}p^2}$$ 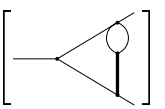 $$= \frac{p^2}{p^2+m^2}\left(\frac{4-D}{2}(4+5\frac{m^2}{p^2})\right.$$ 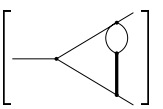 $$+\frac{10-3D}{2}$$ 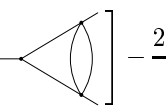 $$-\left.\frac{2-D}{2}\right.$$  $$\Bigg). \quad (5)$$

Here the thick lines represent massive propagators with mass m, the thin lines denote massless propagators and p is the momentum flowing into the vertex. D is the dimension of dimensional regularization. The momentum derivate of the scalar integrals on the left-hand side results in the same integral and simpler integral topologies on the right-hand side. Feeding in analytical results for these simpler integrals, the differential equation can be solved in terms of generalized polylogarithms. All integrals were also checked by using low-momentum expansions.

The second method makes use of numerical integrations based on dispersion relations. A scalar two-loop integral with a self-energy sub-loop as in Fig. 2 (a) can be expressed as [18]

$$T_{N+1}(p_i; m_i^2) = -\int_{s_0}^{\infty} \mathrm{d}s\, \Delta B_0(s, m_N^2, m_{N+1}^2) \int \mathrm{d}^4 q\, \frac{1}{q^2-s}\, \frac{1}{(q+p_1)^2-m_1^2} \cdots \frac{1}{(q+p_1+\ldots+p_{N-1})^2-m_{N-1}^2}, \quad (6)$$

where ΔB_0 is the discontinuity of the scalar one-loop self-energy function. The second integral can be evaluated into a standard N-point one-loop function, leaving the integration over s to be performed numerically. In general, one can also introduce dispersion relations for triangle sub-loops [19], but it is often technically easier to reduce them to self-energy sub-loops by introducing Feynman parameters [20],

$$\begin{gathered}[(q+p_1)^2-m_1^2]^{-1}\,[(q+p_2)^2-m_2^2]^{-1} = \textstyle\int_0^1 \mathrm{d}x\,[(q+\bar{p})^2-\overline{m}^2]^{-2} \\ \bar{p} = x\,p_1+(1-x)p_2, \qquad \overline{m}^2 = x\,m_1^2+(1-x)m_2^2-x(1-x)(p_1-p_2)^2.\end{gathered} \quad (7)$$

This is indicated diagrammatically in Fig. 2 (b). The integration over the Feynman parameters is also performed numerically. As a result, all master integrals for the vertex topologies can be evaluated by at most 3-dim. numerical integrations. Before performing the numerical integrations, possible UV- and IR-divergencies need to be subtracted from the integrals. While this second method is applicable to two-loop vertex corrections with an arbitrary number of mass scales, it is slower and leads to much large expressions than the first method. Nevertheless it provides an important check of the result.

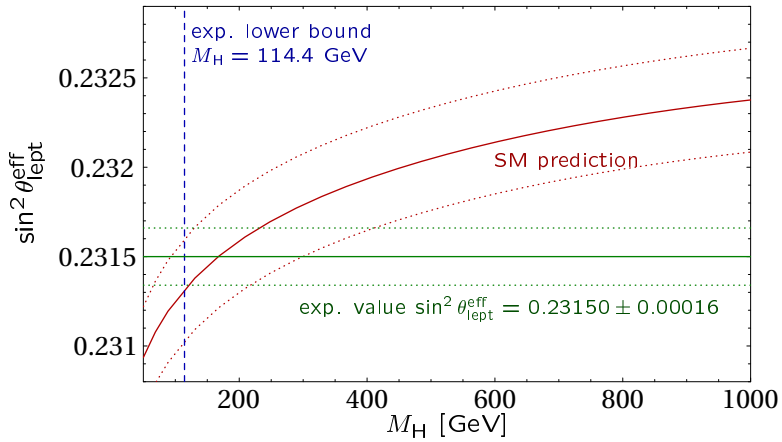

Figure 3: Prediction for $\sin^2\theta^{\rm lept}_{\rm eff}$ including two-loop corrections compared to the current direct experimental measurement, with 1σ bands from experimental input. The chosen input parameters are $M_{\rm Z} = (91.1876 \pm 0.0021)$ GeV, $\Gamma_{\rm Z} = 2.4952$ GeV, $m_{\rm t} = 178.0 \pm 4.3$ GeV, $m_{\rm b} = 4.85$ GeV, $\Delta\alpha(M_{\rm Z}^2) = 0.05907 \pm 0.00036$, $\alpha_{\rm s}(M_{\rm Z}^2) = 0.117 \pm 0.002$, $G_\mu = 1.16637 \times 10^{-5}$ GeV^{-2}.

Special caution is needed for the diagrams with a fermion triangle loop (see the third diagram in Fig. 1), which involve the γ_5 matrix. In dimensional regularization, it is not possible to fulfill the two relations $\{\gamma_\mu, \gamma_5\} = 0$ and $\mathrm{Tr}(\gamma^\alpha\gamma^\beta\gamma^\gamma\gamma^\delta\gamma_5) = 4i\epsilon^{\alpha\beta\gamma\delta}$ simultaneously. As in Ref. [3], the contributions resulting in ϵ-tensors were therefore evaluated in four dimensions, based on the observation that these terms are free of UV-divergencies. Potential soft and collinear divergencies of single diagrams are regulated using a photon mass, with a subsequent careful expansion for zero photon masses.

3. RESULTS

The new result for the fermionic two-loop corrections is combined with corrections of order $\mathcal{O}(\alpha)$, $\mathcal{O}(\alpha\alpha_{\rm s})$ [9], $\mathcal{O}(\alpha\alpha_{\rm s}^2)$ [5] and leading three-loop terms of $\mathcal{O}(\alpha\alpha_{\rm s}^2 m_{\rm t}^4)$ and $\mathcal{O}(\alpha^3 m_{\rm t}^6)$ [6]. Reducible terms of the same order are taken into account, but no resummations are preformed. The most precise prediction of $\sin^2\theta^{\rm lept}_{\rm eff}$ is obtained as a function of the muon decay constant G_μ, from which the W-boson mass is calculated by including the radiative corrections to $M_{\rm W}$ as given in Ref. [2].

Fig. 3 shows the final result for $\sin^2\theta^{\rm lept}_{\rm eff}$ as a function of the Higgs mass compared to the current experimental value. Included in the plot are the error bands due to the uncertainties of the experimental input parameters entering into the theoretical prediction and of the direct measurement of $\sin^2\theta^{\rm lept}_{\rm eff}$. As evident from the figure, the identification of computation and measurement for $\sin^2\theta^{\rm lept}_{\rm eff}$ favor relatively small values for $M_{\rm H}$. With the new two-loop corrections, the best-fit value for $M_{\rm H}$ moved from 148 GeV (using formulae of Ref. [13]) to 168 GeV (for $m_{\rm t} = 178$ GeV).

The numerical result for the leptonic effective weak mixing angle has been published in Ref. [14] as a parametric fitting formula that is accurate in the range 10 GeV $\leq M_{\rm H} \leq$ 1 TeV. It has also been implemented into the newest version 6.42 of the program ZFITTER [21], with some changes recently discussed in Ref. [22], and was used in the latest release of electroweak precision global fits of the Standard Model. The impact of the new result for $\sin^2\theta^{\rm lept}_{\rm eff}$ shifts the 95% confidence level upper bound on the Higgs mass upwards by 23 GeV to 260 GeV [1].

Together with the inclusion of the new two-loop result in the prediction for $\sin^2\theta^{\rm lept}_{\rm eff}$, a assessment of the uncertainties from missing higher order contributions is required. Since for practical purposes $\sin^2\theta^{\rm lept}_{\rm eff}$ is given as a function of the muon decay constant G_μ, it is useful to evaluate the theoretical error for this parametrization, i.e. combining the radiative corrections to $M_{\rm W}$ and the Z vertex. A simple method to estimate the higher order uncertainties assumes that the perturbation series follows roughly a geometric progression. This presumption implies relations like $\mathcal{O}(\alpha^2\alpha_{\rm s}) = \mathcal{O}(\alpha^2)/\mathcal{O}(\alpha)\,\mathcal{O}(\alpha\alpha_{\rm s})$. With this method one obtains the following errors for $M_{\rm H}$ between 10 and 1000

GeV in units of 10^{-5}: between 2.3 and 2.0 for the $\mathcal{O}(\alpha^2\alpha_s)$ contributions beyond the leading m_t^4 term, between 1.8 and 2.5 for $\mathcal{O}(\alpha^3)$, between 1.1 and 1.0 for $\mathcal{O}(\alpha\alpha_s^3)$ and between 1.7 and 2.4 for $\mathcal{O}(\alpha^2\alpha_s^2)$. The missing bosonic $\mathcal{O}(\alpha^2)$ corrections cannot be appraised from geometric progression. However, considering they have a prefactor α^2 but no specific enhancement factor, they are estimated to be about 1.2×10^{-5}. To account for possible deviations from the geometric series behavior, an overall factor $\sqrt{2}$ was included to arrive at a total error of $\delta_{\rm th}\sin^2\theta_{\rm eff}^{\rm lept} = 4.9 \times 10^{-5}$.

Alternatively, the error from a higher-order QCD loop can be assessed by varying the scale of the strong coupling constant α_s or the top-quark mass m_t in the $\overline{\rm MS}$ scheme in the highest available perturbation order. The scale variation leads to an error estimate of 0.1 to 3.9×10^{-5} for the $\mathcal{O}(\alpha^2\alpha_s)$ corrections and of less than 10^{-6} for the $\mathcal{O}(\alpha\alpha_s^3)$ contributions. These numbers are of the same order as the estimated errors from the geometric progression method, so that the total error given above seems to be fairly reliable.

The new error estimate was used in the latest electroweak global fits [1] and lead to a reduction of the width of the well-known *blue band*, which indicates the theoretical error in the indirect determination of the Higgs mass.

4. CONCLUSIONS

In this contribution, recent progress in the calculation of higher-order corrections to the most important electroweak precision observables and their impact on the indirect determination of the Higgs mass was reported.

The complete fermionic $\mathcal{O}(\alpha^2)$ corrections to the leptonic effective weak mixing angle $\sin^2\theta_{\rm eff}^{\rm lept}$ have been calculated and numerical results were presented. As an additional check, the computation of the two-loop vertex integrals was performed with two independent methods. The new result, together with an estimate of the remaining theoretical error, was included in the latest version of the program ZFITTER and used for the latest global electroweak fits of the Standard Model.

The calculation of the remaining bosonic electroweak two-loop corrections is currently in progress and will be available soon [23]. Furthermore, we are working on adapting the new results for quark final states, where particular attention has to be paid to the $Zb\bar{b}$ vertex, since it includes additional massive top-quark propagators [23].

Acknowledgments

The authors are grateful to G. Weiglein for valuable contributions, comments and communications concerning this project. M. C. was supported by the Sofja Kovalevskaja Award of the Alexander von Humboldt Foundation sponsored by the German Federal Ministry of Education and Research. M. A. and M. C. were supported by the Polish State Committee for Scientific Research (KBN) for the research project in years 2004-2005.

References

[1] The LEP Electroweak Working Group and the SLD Electroweak and Heavy Flavour Groups, hep-ex/0412015.
[2] M. Awramik, M. Czakon, A. Freitas and G. Weiglein, Phys. Rev. D **69**, 053006 (2004).
[3] A. Freitas, W. Hollik, W. Walter and G. Weiglein, Phys. Lett. B **495**, 338 (2000) [Erratum-ibid. B **570**, 260 (2003)], Nucl. Phys. B **632**,189 (2002) [Erratum-ibid. B **666**, 305 (2003)]; M. Awramik and M. Czakon, Phys. Lett. B **568**, 48 (2003).
[4] M. Awramik and M. Czakon, Phys. Rev. Lett. **89**, 241801 (2002); A. Onishchenko and O. Veretin, Phys. Lett. B **551**, 111 (2003); M. Awramik, M. Czakon, A. Onishchenko and O. Veretin, Phys. Rev. D **68**, 053004 (2003).
[5] K. G. Chetyrkin, J. H. Kühn and M. Steinhauser, Phys. Rev. Lett. **75**, 3394 (1995).
[6] M. Faisst, J. H. Kühn, T. Seidensticker and O. Veretin, Nucl. Phys. B **665**, 649 (2003).
[7] A. Sirlin, Phys. Rev. D **22**, 971 (1980);
W. J. Marciano and A. Sirlin, Phys. Rev. D **22**, 2695 (1980) [Erratum-ibid. D **31**, 213 (1980)].

[8] G. Degrassi and A. Sirlin, Nucl. Phys. B **352**, 342 (1991); P. Gambino and A. Sirlin, Phys. Rev. D **49**, 1160 (1994).

[9] A. Djouadi and C. Verzegnassi, Phys. Lett. B **195**, 265 (1987); A. Djouadi, Nuovo Cim. A **100**, 357 (1988); B. A. Kniehl, Nucl. Phys. B **347**, 86 (1990); F. Halzen and B. A. Kniehl, Nucl. Phys. B **353**, 567 (1991); B. A. Kniehl and A. Sirlin, Nucl. Phys. B **371**, 141 (1992), Phys. Rev. D **47**, 883 (1993); A. Djouadi and P. Gambino, Phys. Rev. D **49**, 3499 (1994) [Erratum-ibid. D **53**, 4111 (1996)].

[10] K. G. Chetyrkin, J. H. Kühn and M. Steinhauser, Nucl. Phys. B **482**, 213 (1996).

[11] J. J. van der Bij and F. Hoogeveen, Nucl. Phys. B **283**, 477 (1987).

[12] R. Barbieri, M. Beccaria, P. Ciafaloni, G. Curci and A. Vicere, Phys. Lett. B **288**, 95 (1992) [Erratum-ibid. B **312**, 511 (1993)], Nucl. Phys. B **409**, 105 (1993); J. Fleischer, O. V. Tarasov and F. Jegerlehner, Phys. Lett. B **319**, 249 (1993), Phys. Rev. D **51**, 3820 (1995).

[13] G. Degrassi, P. Gambino and A. Sirlin, Phys. Lett. B **394**, 188 (1997).

[14] M. Awramik, M. Czakon, A. Freitas and G. Weiglein, Phys. Rev. Lett. **93**, 201805 (2004).

[15] K. G. Chetyrkin and F. V. Tkachov, Nucl. Phys. B **192**, 159 (1981); S. Laporta and E. Remiddi, Phys. Lett. B **379**, 283 (1996); S. Laporta, Int. J. Mod. Phys. A **15**, 5087 (2000).

[16] M. Czakon, DiaGen/IdSolver library (unpublished).

[17] A. V. Kotikov, Phys. Lett. B **259**, 314 (1991); E. Remiddi, Nuovo Cim. A **110**, 1435 (1997).

[18] S. Bauberger, F. A. Berends, M. Böhm and M. Buza, Nucl. Phys. B **434** (1995) 383.

[19] S. Bauberger and M. Böhm, Nucl. Phys. B **445** (1995) 25. A. Czarnecki, U. Kilian and D. Kreimer, Nucl. Phys. B **433**, 259 (1995); A. Frink, B. A. Kniehl, D. Kreimer and K. Riesselmann, Phys. Rev. D **54**, 4548 (1996); A. Frink, U. Kilian and D. Kreimer, Nucl. Phys. B **488**, 426 (1997).

[20] A. Ghinculov and J. J. van der Bij, Nucl. Phys. B **436** (1995) 30.

[21] A. B. Arbuzov, M. Awramik, M. Czakon, A. Freitas, M. W. Grünewald, K. Mönig, S. Riemann, T. Riemann, *ZFITTER: a semi-analytical program for fermion pair production in e^+e^- annihilation, from version 6.21 to version 6.42*, DESY 05–34, FERMILAB–Pub–05–256–T, submitted to Comp. Phys. Commun. [`http://www-zeuthen.desy.de/theory/research/zfitter/`].

[22] A. Freitas and K. Mönig, Eur. Phys. J. C **40**, 493 (2005).

[23] M. Awramik, M. Czakon and A. Freitas, in preparation.